Precision Machining of Ceramic Materials

PETER BLAKE, THOMAS BIFANO,* THOMAS DOW, and RONALD O. SCATTERGOOD

North Carolina State University, Precision Engineering Center, Raleigh, NC 27695-7910

Machining processes that can hold submicrometer tolerances and produce surface finishes better than 10 nm are at the frontier of precision fabrication, yet these are the standard specifications for many advanced optical, electronic, and mechanical components. Currently, a new generation of precision machines and fabrication processes are evolving to meet this need. The principles governing the design of these machines differ from those used in conventional machining. Thermal stability, vibration isolation, kinematic support, feedback control, and metrology frames are critical elements in the development of precision machines.

In addition, the manufacture of precision parts hinges on an understanding of the mechanics of the material-removal process. Since the characteristic machining chip dimensions are on the order of ≤ 1 μm, the effects of grain boundaries, local imperfections, and dislocation mobility influence the chip formation that, in turn, affects the topography and stress state of the workpiece. When the workpiece is a ceramic, an additional concern is the regime of material removal, i.e., whether chip formation occurs in a ductile process (plastic deformation) or in a brittle process (crack propagation).

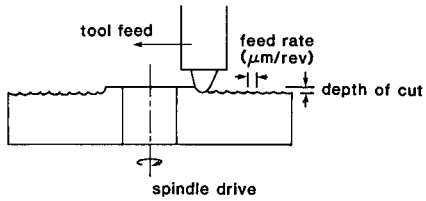

Fig. 2. Facing operation on PAUL.

Materials with a relatively low fracture toughness normally respond to applied forces by the generation and propagation of cracks. However, under the localized-contact conditions that prevail for surface-machining conditions, this need not be the case. Precision machining is in many respects similar in nature to tribological processes associated with abrasion and abrasive wear.[1,2] Figure 1 illustrates the relevant material-removal mechanisms discussed by Evans and Marshall.[3] Above a critical normal load, P_n, stresses in the plastic zone in Fig. 1(*A*) will generate fracture damage in the form of lateral and median crack systems. Such fracture damage cannot be tolerated for precision surface finishing. Below a critical load, which may be quite small, a ductile regime for material removal via plastic cutting mechanisms can be achieved, as shown in Fig. 1(*B*). It is this "ductile regime" that is central to precision-finishing processes. Although a large body of data exists for fracture-damage processes under indentation-type loading conditions,[4] the actual mechanisms that underlie ductile-regime precision-finishing technologies are poorly understood at the present time. Current research efforts involving expertise in materials, mechanical-system design, and metrology are being applied to gain new insight into the limits, phenomenology, and mechanisms pertinent to precision-finishing technologies.

To machine hard materials in a ductile regime, the forces between the tool and the workpiece must be kept below critical values. Obtaining precise dimensional control, on the other hand, requires an exceptionally stiff machine so that infeeding the tool translates into chip re-

*Present address: Dept. of Mechanical Engineering, Boston University, Boston, MA 02255.

Supported by the Office of Naval Research under Contract No. ONR-N00014-86-K-0681 and by industrial sponsors of the Precision Engineering Center at North Carolina State University.

Reprinted with permission from the Proceedings of the Intersociety Symposium on Machining of Advanced Ceramic Materials and Composites, held April 1987.

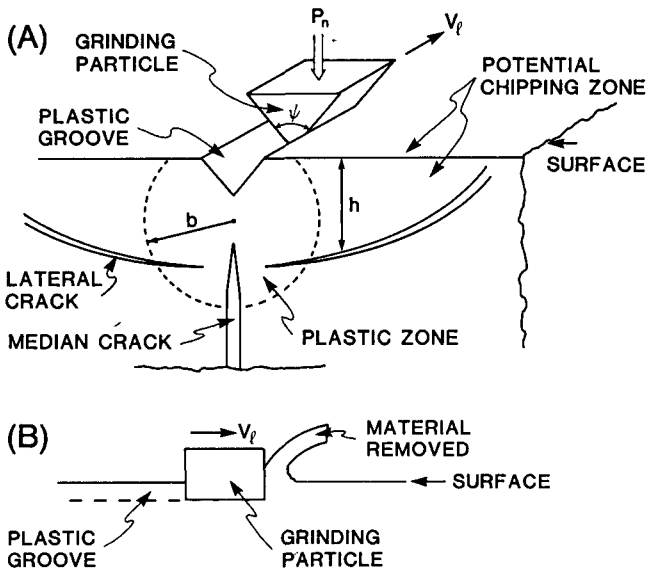

Fig. 1. Fracture processes[3]: (*A*) lateral fracture mechanism; (*B*) plastic cutting mechanism.

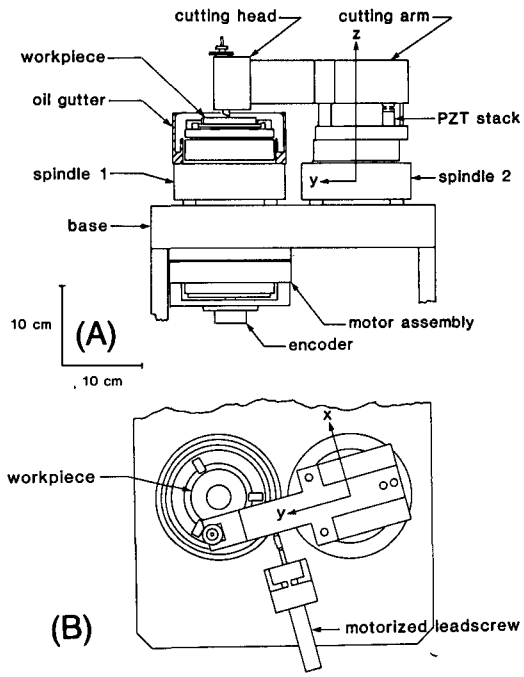

Fig. 3. Diagram of PAUL.

Table I. PAUL Parameters

Workpiece spindle	Vertical error	Lateral error
Runout	50 nm	50 nm
Coning	30 nm	15 nm
Tool spindle		
Runout	50 nm	50 nm
Coning	8 nm	15 nm
Total spindle errors	138 nm	130 nm
Stiffness between tool holder and workpiece spindle		8.8×10^6 N/m
Thermal growth tool/workpiece position		40 nm/°C
Workpiece spindle speed		0–5000 rpm

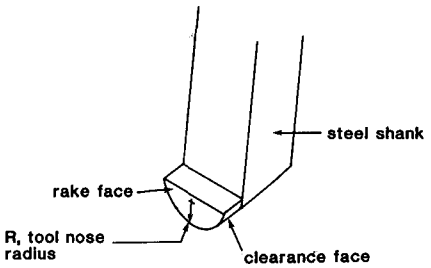

Fig. 4. Diamond tool.

moval from the workpiece, not flexure of the machine. Thus, two requirements for precision machining hard materials are low cutting forces and high machine rigidity. For these goals to be accomplished simultaneously, submicrometer control of the tool infeed with respect to the workpiece is also required. Therefore, in addition to the need for an actuator with submicrometer resolution, the total effects of thermal drift, vibration, and spindle runout must be reduced to acceptable levels or compensated.

A single-point diamond-turning machine and a diamond-grinding machine were both designed using the above guidelines. For stiffness and low runout, both machines use hydrostatic air bearings for the primary machine motion. These bearings exhibit <0.05-μm axial runout, with an axial stiffness of 1.2×10^8 N/m at the point of tool contact. For tool-depth adjustment, both systems incorporate stiff piezoelectric actuators capable of high-speed motion over 12.5 μm, with a resolvable motion increment of 12.5 nm.

To eliminate thermal-expansion problems, both machines are located in a temperature-controlled room regulated to ±0.1°C. For vibration elimination, each machine is mounted on a vibration-isolation table that effectively attenuates environmental disturbances of >5 Hz.

Single-Point Diamond Turning

The Precision Engineering Center's research lathe uses a vertical-axis, air-bearing spindle to rotate the workpiece. The tool holder is mounted on a second air-bearing spindle, instead of a linear slide. Driven slowly, this allows the tool to sweep across the face of the workpiece toward its center. This design gives rise to the acronym PAUL—parallel-axis ultraprecision lathe. Figure 2 is a cross-sectional view of the tool–workpiece setup. Figure 3 shows the lathe's construction, which was described by Falter.[5] The tool can be adjusted vertically with the lead–zirconium–titanate (PZT) stack to control the depth of cut and can be driven horizontally at different feed rates.

The major sources of machine error in the design are bearing-error motions, misalignment of the spindle axes, thermal expansion, and vibration. Table I summarizes the relevant machine parameters.

The tool is a single-crystal diamond mounted on a steel shank (Fig. 4). One surface, the rake face, is polished flat. The clearance face meets the rake face at an included angle of 83°. The tool-nose profile is circular and cuts a groove with circular cross section. The tool can be rotated around the nose profile to present new, unworn sections of the cutting edge to the surface. The cutting edge is so sharp that an edge radius is undetectable by optical microscopy.

The turned surface has a topography formed by the feed grooves. If the tool removed only the material in its path and, in addition, never deviated in its path from a straight and level line, the resultant scalloped surface would have an ideal peak-to-valley roughness, R_t, equal to

$$R_t = \frac{f^2}{8R} \qquad (1)$$

where f is the feed per revolution and R is the tool-nose radius.

A typical finish cut for metal optics may use a feed of 6 μm, a depth of cut of 2 μm and a tool with nose radius of 0.762 mm (0.030 in.). This would leave a scalloped surface whose peak-to-valley roughness, R_t (ideal), would equal 6 nm. The average slope would be 0.1°. Such roughness values make it clear that if the cutting process is precise, the surface will be specular.

Geometry of the Diamond Turning Process

Most of the effort in precision machining goes to ensuring that the tool will travel in the path designed for it, within a defined margin of error. In the present study, interest is focused largely on the surface roughness within individual feed marks. Roughness on this scale produces high-angle scatter and thus determines whether a finish looks specular or matte.

Figure 5 illustrates the geometry of the chip-formation process, simplified to a two-dimensional (orthogonal) model. The material within the region enclosed by the undeformed chip thickness, t, will be separated from the workpiece by the diamond tool. In the machining of ceramics, the deformation processes within the material-removal zone are as yet poorly understood.

The true cross section of the undeformed chip of a finish cut is shown to scale in Fig. 6. This view is along a direction parallel to the cutting path and shows that the thickness of the cut, t, varies almost linearly across the width of the chip. A formula for the maximum chip thickness can be developed from the geometry of the cutting process, which in-

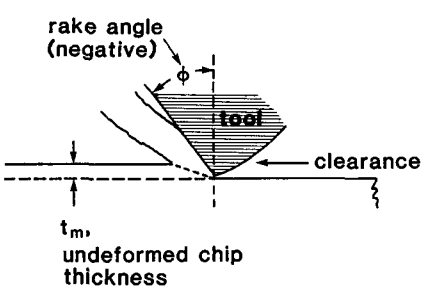

Fig. 5. Chip-formation process.

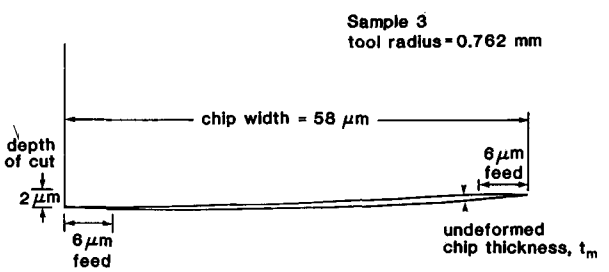

Fig. 6. Cross section of undeformed chip.

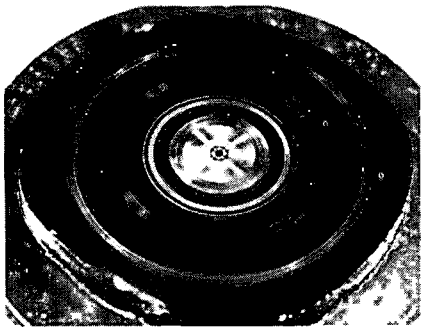

Fig. 7. Germanium disk showing the finishes produced by 16 depth-and-feed conditions. Notice the smooth areas, the light-scattering areas of pitting, and four-fold symmetric pattern of severe pitting. The four-fold arms are centered on axes displaced from the <110> axes by 8°.

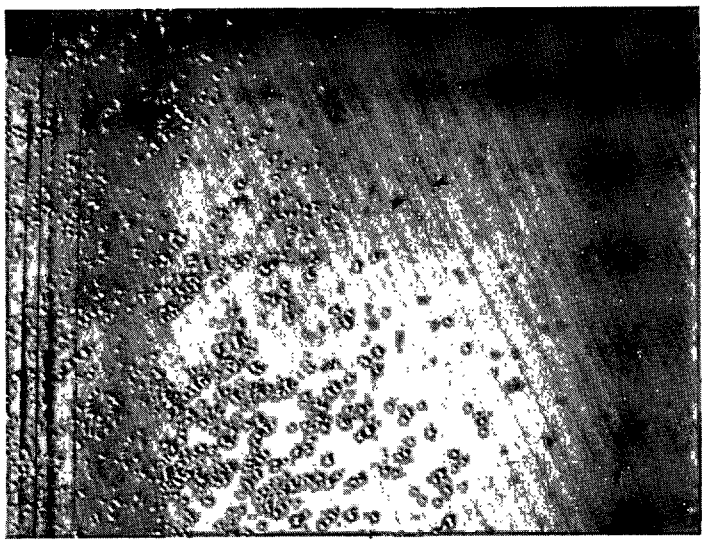

Fig. 8. Pits produced in the surface by a 2.25-μm depth of cut and 5.83-μm feed. Area between the arrows is one feed. (1000×)

volves the tool-nose radius, R; the feed rate per revolution, f; and the depth of cut, d.

$$t_m = f \cos^{-1}\left[1-\frac{d}{R}\right] \quad (2)$$

The chip width is given by

$$W = R \cos^{-1}\left[1-\frac{d}{R}\right]+\frac{f}{2} \quad (3)$$

For example, in a typical cut with depth and feed both 2 μm, and $R=3.2$ mm, the maximum thickness of the undeformed chip is 1/30 of the depth of cut, and the width of the chip is >50 times greater than the feed. The tool will be removing material from above any point in the finish surface during each of its 50 passes over that point.

Diamond-Turning Studies

Optical-grade germanium single crystal, in the form of a 2.5-cm- (1.0-in.-) radius disk, was centered on a holder that can be mounted on the lathe. The crystal was ground parallel and then etched to remove grinding damage. It was oriented with the (100) direction facing up, and this face was machined on the lathe in a facing operation. Deionized water was used as the lubricant/coolant. In the initial tests, facing cuts were made at 1000 rpm, giving a cutting speed of 2.5 ± 0.5 m/s. The rake angle was −1°.

The first series of cuts taken illustrates the type of surface damage that occurs. Much of the face was very smooth, but there were four arms of high light scatter in the form of a four-fold symmetric cross through the center (Fig. 7). These regions were composed of 0.1-μm-deep pits (Fig. 8). In subsequent trials, on surfaces oriented on the (100), (110), and (111) planes, the pitting occurred while the tool passed within a few degrees of the <110> directions. For the (110) samples, pitting also occurs in the <100> direction.

The surface profile in the unpitted areas was measured with a stylus profilometer.[†,6] The peak-to-valley roughness, R_t, over sample lengths of 75 μm, averaged 8 nm, and over lengths of 12.5 μm (≈8 feeds), it was 1.6 nm. The waviness over longer sample lengths was larger because of unwanted tool motion in the tool-feed mechanism.

Scanning electron micrographs of the machining debris reveal chips from machining germanium that appear quite similar to metal chips. Figures 9 (*A*) and (*B*) compare germanium chips to copper chips for given machining conditions.[7] Figure 10 shows germanium chips and the ribbon-like continuity which is expected for ductile material flow. It can be concluded from these experiments that ductile-regime deformation is possible when machining germanium. Further experiments are required to clarify the range of parameters which define the limits of the ductile regime.

To test the effect of cutting depth and feed, a matrix of experiments—three depths and three feeds—was performed. Table II displays the results. The presence and extent of pitting is the criterion used in analyzing the results in Table II. As conditions worsen, the smooth surface gives way to one with scattered pitting in the four symmetric regions, then to concentrated pitting over 360°. Careful study of Table I reveals that smooth surface fin-

[†]Talystep, Rank Precision Industries, Inc., Des Plaines, IL.

Fig. 9. Chips of (*A*) germanium machined at 1.5-μm feed, 0.5-μm depth of cut, and 0.025-μm t_m and (*B*) copper machined at 6.3-μm feed, 2.3-μm depth of cut, and 0.5-μm t_m. (bars=5 μm)

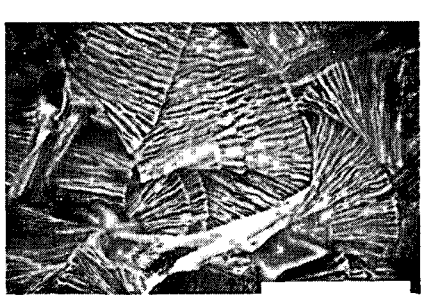

Fig. 10. Machining chips of germanium show ribbon-like continuity. (bar=10 μm)

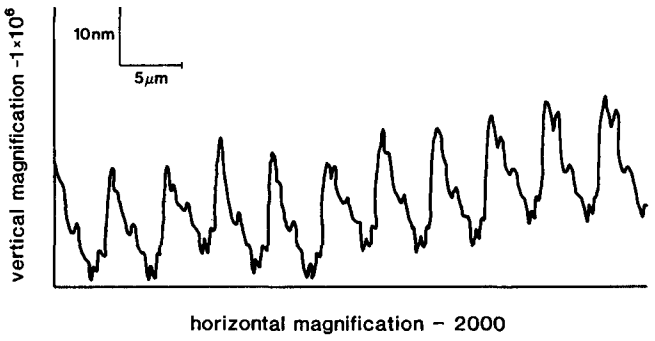

Fig. 11. Profilometer diagram of turned germanium surface. Depth of cut=4 μm; feed=6 μm.

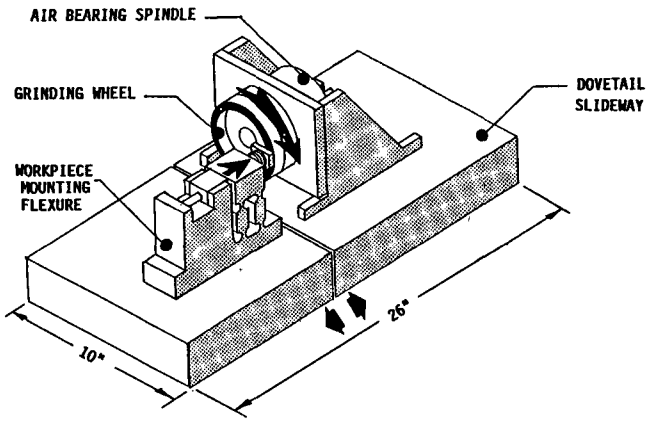

Fig. 12. PEGASUS grinder schematic.

ishes resulted when the maximum chip thickness was <0.1 μm.

Very recent results[8] have in fact revealed that damage created at the forward edge of the tool is frequently removed by the final passes of the tool over a spot on the final surface. There is indeed a critical chip thickness, but it is not the maximum chip thickness, t_m, as herein described. The critical chip thickness, t_c, is that chip thickness for which no fracture or pitting occurs during material removal; if the feed per revolution is set such that there are several passes of the tool with chip thickness less than t_c, the final surface will be unpitted. A surprising result is that the feed per revolution is the important parameter and that large depths of cut (>500 μm) can leave a smooth surface.

It is interesting to note that even a badly worn tool can remove the material in an apparently ductile fashion. The nicks and grooves in the tool edge create roughness within the groove that leads to a diffraction effect from the otherwise specular surface. But Fig. 11, the profilometer image of the surface, shows that the tool edge is replicated quite faithfully from groove to groove.

This faithful replication will be used in a new technique for monitoring tool-edge wear: the witness-sample method.[9,10] At the beginning and end of each trial, the tool is slowly plunged into the surface to twice the finish depth of cut. Alternatively, a copper witness sample can be used. The shape of the groove is a signature of the tool, giving a record of tool nicks and a measure of the recession, through wear, of the cutting edge from its original nose profile.

Diamond Grinding

Using the machine guidelines already described, the precision engineering grinding apparatus for superfinishing ultrahard surfaces (PEGASUS) was designed and built. The machine operates in a plunge-grinding mode, in which the workpiece is fed in a normal direction to the surface of the 0.64-cm-wide rim of a cup-grinding wheel.

The grinding wheels used on this apparatus are type 6A2, 10-cm-diameter cup wheels with diamond grain size of 4 to 8 μm and concentration values of 75 (3.3 carats/cm³). Bonding matrices for the diamond grains are either metal or resin. The grinding wheel is mounted on a 10-cm-diameter air-bearing spindle driven by a variable speed (0 to 5000 rpm) dc motor. The grinding-wheel spindle is fixed to a 60 cm by 25 cm scraped dovetail slideway.

The workpiece is mounted to the face of a piezoelectric actuator capable of 12.5 μm of linear infeed motion, at a speed to 12.7 cm/s and a resolution of 12.5 nm. The base of the piezoelectric actuator is attached to a clamped flexure assembly that is manually actuated via a leadscrew (3.15 threads/mm) for coarse positioning. These flexures are clamped during the actual grinding. The linear range of this coarse-positioning system is ≈0.5 mm with a resolution of 0.5 μm. The entire flexure/PZT/workpiece assembly is mounted on a movable saddle on the dovetail slideway and has a 15-cm linear range. Figure 12 illustrates the PEGASUS design, whereas Fig. 13 is a photograph of the apparatus. Table III summarizes the relevant machine parameters.

The spindle motor drives the spindle via a flat belt. The stiffness of the appa-

Table II. t_m versus Depth of Cut and Feed per Revolution

Sample	depth (μm)	feed (μm)	t_m (μm)	Description of finish
I_2	2.3	2.1	0.08	Smooth
I_3	2.3	4.2	0.16	Scattered pitting only in 4 regions (±7° wide)
I_4	2.3	5.9	0.22	Scattered pitting over 360°
II_2	1.1	2.1	0.06	Smooth
II_3	1.1	4.2	0.11	Scattered pitting only in 4 regions
II_4	1.1	5.9	0.15	Severe pitting over 360°
III_2	0.46	2.1	0.04	Smooth
III_3	0.46	4.2	0.07	Smooth
III_4	0.46	5.9	0.10	Smooth

Table III. PEGASUS Parameters

Stiffness wheel/workpiece interface	53×10^6 N/m
Axial wheel runout	0.25 μm per revolution
Workpiece-positioning resolution	12.5 nm
Feed rate	0–12.5 cm/s
Wheel speed	0–5000 rpm
Lubrication	Variable-pressure air-entrained fluid or flood types
Computer-controlled constant-force or constant-infeed grinding modes	

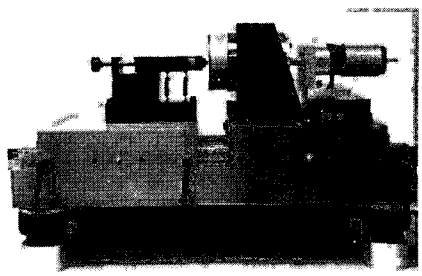

Fig. 13. PEGASUS grinder photograph.

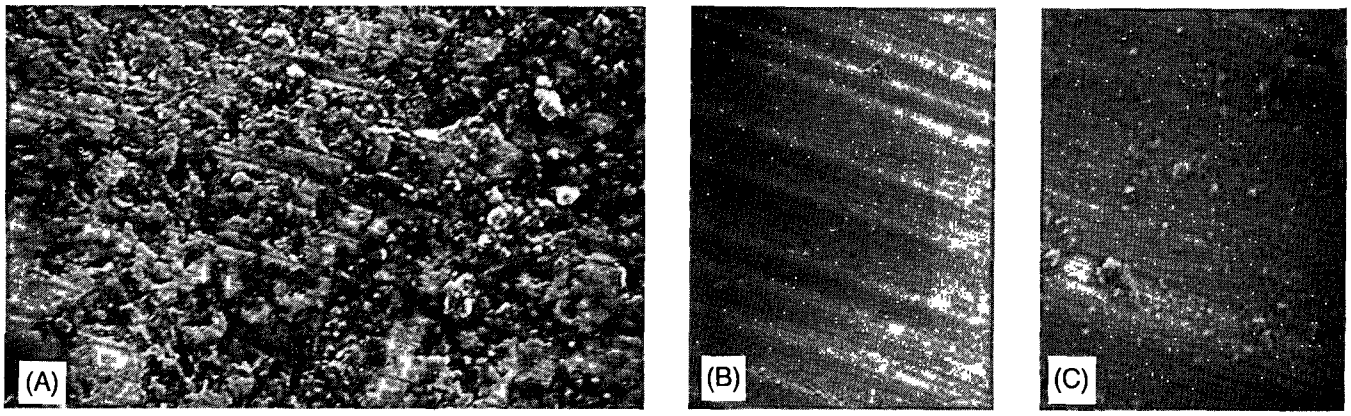

Fig. 14. Silicon carbide plunge ground on (*A*) a conventional grinder (1000×), (*B*) on PEGASUS (1000×), and (*C*) also on PEGASUS (5000×).

ratus at the wheel/workpiece interface is $\approx 53\times10^6$ N/m. This value far exceeds that of standard grinders and is within the bounds typically specified for precision machining.

Wheel truing is necessary to minimize the surface runout of the grinding wheel face. Runout of the wheel surface causes fluctuations in the grinding force, which can potentially affect the ductility of the grinding process. These runout-induced force variations are magnified by the rigidity of the PEGASUS apparatus.

For example, a 1-μm surface runout of the grinding wheel causes >50 N of variation in the normal cutting force. The other contributors to force variability (bearing runout and vibration) are small by comparison. The goal of the truing effort, then, is to reduce the wheel runout to a level that is comparable to the combined effects of these other sources of runout (≈0.05 μm). Recently developed techniques[8] reduced the face runout to 0.12 μm, peak to valley.

Ductile-Regime Grinding

To demonstrate its potential, the PEGASUS machine was used to grind a sample of reaction-bonded silicon carbide.[‡] A parallel plunge grind was made on this same sample using a conventional grinding machine. A comparison of the results of these two experiments should qualitatively demonstrate the potential for a brittle–ductile transition, given an adequate control of the machining parameters. Figure 14 dramatically illustrates the difference between a brittle material removal mechanism and a ductile one. Figure 14(*A*) is the sample ground by a conventional grinder,[§] whereas Figs. 14(*B*) and (*C*) illustrate the same sample ground on the PEGASUS machine. The parallel lines on these photomicrographs (particularly evident in the sample ground on the PEGASUS machine) are grooves from which the diamond grains have ductilely removed material. The irregularly shaped areas dominating the conventionally ground sample are areas of brittle fracture and cracking, as was indicated schematically in Fig. 1. Many of the grinding parameters were different for the two systems. The infeed for the conventional grinder was manually actuated, with a resolution no better than 2.5 μm, and exhibits considerable stick/slip in its motion. Additionally, the conventional grinder exhibits >12.5 μm of axial runout. Because of these differences, this test yields little quantitative information concerning the effects of individual machine parameters. Nevertheless, the motivation for researching ductile-regime grinding is clearly demonstrated, as is the potential of the PEGASUS machine to achieve this regime.

An attempt is being made to isolate the parameters of ductile-regime grinding for specific materials. The protocol for this experiment is to keep certain machine variables and workpiece-material properties constant, while individually varying other grinding parameters. The goal is to identify the effects of these parameters on the ductility of the grinding process. The fixed conditions are: contact stiffness, 53×10^6 N/m; overall depth of cut, 30 μm; wheel grain size, 4 to 8 μm, 3.3 carats/cm³; and infeed mode, constant, computer-feedback-controlled. The variable conditions are: workpiece-material feed rate, 0.25 to 25 nm per revolution; wheel speed, 100 to 5000 rpm; lubricant, oil, water, ethanol, or none; and wheel bond, resin or metal.

Despite that these experiments are incomplete, a range of grinding ductility was observed when certain machining conditions were varied. Figure 15 illustrates the brittle–ductile transition through a series of SEM micrographs (5000×). These micrographs are of fused-silica samples ground at infeed rates from 37.5 to 1.5 nm per revolution. A significant improvement in surface quality can be seen for progressively smaller infeed rates. Profile measurements along the grinding

[‡]Noralide NC-430, Norton Co., Worcester, MA.
[§]Of type supplied by Cincinnati Milacron, Products Div., Cincinnati, OH.

Fig. 15. Microground fused-silica surface with infeed rates of (*A*) 37.5, (*B*) 7.5, and (*C*) 1.5 nm per revolution. (bars=10μm)

grooves of these samples yielded a remarkable difference: the more-ductilely ground sample has a peak-to-valley roughness of ≈50 nm, whereas a corresponding groove on the less-ductilely ground sample has a peak-to-valley roughness of >1 μm, a 20:1 difference in smoothness.

As the experimental grinding research progresses, the critical influences in ductile-regime grinding of hard materials will be defined in terms of both grinding parameters and material properties. Additionally, the mechanics of the grinding contact will be investigated, including the effects of temperature, grain dynamics, and local stresses at the wheel–workpiece contact.[11–13] As a first approximation, appropriate extensions of previously reported scratch-and-indentation analyses will be made.[14–16] Finally, the analysis research will include an investigation of the mechanisms involved in both ductile and brittle material removal in hard materials.

References

[1]D. B. Marshall, A. G. Evans, B. T. Khuri Yakub, J. W. Tien, and G. S. Kino, "The Nature of Machining Damage in Brittle Materials," *Proc. R. Soc. London, A*, **385**, 461 (1983).

[2]H. P. Kirchner and J. C. Conway, Jr., "Mechanisms of Material Removal"; p. 53 in Machining of Ceramic Materials and Components, Vol. 17. American Society of Mechanical Engineers, New York, 1985.

[3]A. G. Evans and D. B. Marshall,"Wear Mechanisms in Ceramics"; p. 439 in Fundamentals of Friction and Wear. Edited by D. A. Rigney. American Society for Metals, Metals Park, OH, 1980.

[4]B. R. Lawn and T. R. Wilshaw, "Indentation Fracture Mechanics of Brittle Materials—A Review," *J. Mater. Sci.*, **10**, 1049 (1975).

[5]P. J. Falter and T. A. Dow, "Design and Performance of a Small-Scale Diamond-Turning Machine"; presented at 1st American Society for Precision Engineering Conference, Dallas, TX, Nov. 5–7, 1986.

[6]J. M. Bennett and J. H. Dancy, "Stylus Profiling Instrument for Measuring Statistical Properties of Smooth Optical Surfaces," *Appl. Opt.*, **20**, 1785 (1981).

[7]P. Blake and R. O. Scattergood, "Chip Topography of Diamond-Turned Ductile Metals"; unpublished work.

[8]P. Blake, T. Bifano, R. O. Scattergood, and T. Dow, "Ductile-Regime Machining of Ceramics"; unpublished work.

[9]C. Syn, J. S. Taylor, and R. R. Donaldson, "Diamond Tool Wear versus Cutting Distance on Electroless Nickel Mirrors"; unpublished work.

[10]H. H. Hurt, "Crystallographic Effects in Diamond Tool Wear"; unpublished work.

[11]J. Yoshioka, F. Hashimoto, M. Miyashita, A. Kanai, T. Abo, and M. Daito, "Ultraprecision Grinding Technology for Brittle Materials: Application to Surface and Centerless Grinding Processes"; pp. 209–27 in Milton Shaw Grinding Symposium Proceedings, Vol. 16. American Society of Mechanical Engineers, New York, 1985.

[12]L. E. Chaloux, "Diamond Grinding of Optical Surfaces on Brittle Materials"; presented at the 1st Annual Precision Engineering Conference at North Carolina State University, Raleigh, NC, November 1986.

[13]S. B. Toh and R. McPherson, "Fine-Scale Abrasive Wear of Ceramics by a Plastic Cutting Process"; presented at the 2nd International Conference on the Science of Hard Materials, Rhodes, Greece, 1986.

[14]M. Huerta and S. Malkin, "Grinding of Glass: The Mechanics of the Process," *J. Eng. Ind.*, **98**, 459–67 (1976).

[15]T. N. Loladze, B. I. Batiashvili, and G. L. Mamulashvili, "Precision Grinding of Piezoquartz, Piezoceramics, and Monocrystalline Silicon," SME Tech. Pap. No. MR 84-543, 1984.

[16]A. Broese van Groenov, N. Maan, and J. B. D. Veldkamp, "Single-Point Scratches as a Basis for Understanding Grinding and Lapping, "*NBS Spec. Publ.* No. **562**, Oct. 1979. ■